Journal of the Meteorological Society of Japan, Vol. 93, No. 2, pp. 229–244, 2015
DOI:10.2151/jmsj.2015-013

Role of Siberian Land-Atmosphere Coupling in the Development of the August Okhotsk High in 2008

Shinji MATSUMURA

Faculty of Environmental Earth Science, Hokkaido University, Sapporo, Japan

Koji YAMAZAKI

National Institute of Polar Research, Tachikawa, Japan
Faculty of Environmental Earth Science, Hokkaido University, Sapporo, Japan

and

Tomonori SATO

Faculty of Environmental Earth Science, Hokkaido University, Sapporo, Japan

(Manuscript received 13 May 2013, in final form 17 December 2014)

Abstract

We investigate the formation mechanism of the summer Okhotsk High (OH) in terms of the land-atmosphere coupling in Siberia. A reanalysis data indicates that the formation mechanism of the OH clearly differs between early and late summer because it changes from a nearly barotropic to a baroclinic structure with seasonal changes. Then, we assess the influence of springtime snow cover on the formation of the late summer OH with the baroclinicity using a regional climate model. The model performs well in reproducing the land-atmosphere coupling in eastern Siberia and the OH in August 2008, when abnormal weather prevails in Japan, in conjunction with the intensively developed OH. The August OH develops with a distinct baroclinic structure owing to increased surface heating, which is related to land-atmosphere coupling in response to reduced spring snow cover in eastern Siberia. The land-atmosphere coupling can help to reinforce and maintain the baroclinic structure through surface heating, forming strong surface anticyclone to the southeast over the Sea of Okhotsk. Our results suggest that the late summer OH is a regional climate system that involves coupling among the atmosphere, the cool ocean, and the warm land surface.

Keywords Okhotsk High; snow cover; eastern Siberia

1. Introduction

The Sea of Okhotsk is a cool ocean bounded to the north (far-eastern Siberia) and west (eastern Siberia) by land masses that remain warm in summertime. A vast area of eastern Siberia is covered by boreal forest on continuous permafrost, where snowmelt water and rainfall infiltrate the soil that thaw the frozen soil during the warm season and are stored as ice throughout the cold season. Boreal forests along 60°N in northern Eurasia are created and maintained by warm seasonal rainfall which is, in turn, caused by water vapor fluxes associated with transient distur-

Corresponding author: Shinji Matsumura, Faculty of Environmental Earth Science, Hokkaido University, Kita 10-Jo Nishi 5, Kita-ku, Sapporo 0060-0810, Japan
E-mail: matsusnj@ees.hokudai.ac.jp

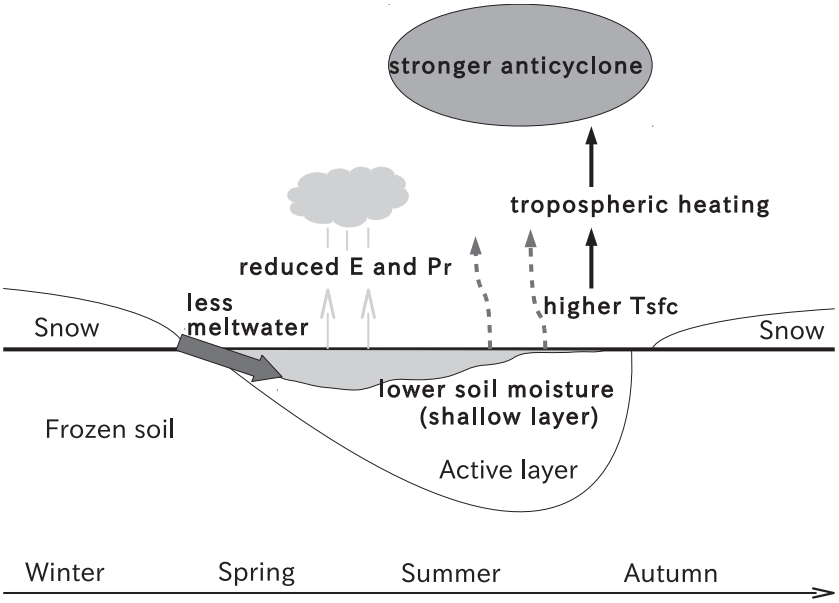

Fig. 1. Schematic diagram of seasonal changes in early-snowmelt years from winter to autumn in eastern Siberia. E: evaporation, P_r: precipitation, and T_{sfc}: surface air temperature (Matsumura and Yamazaki 2012).

bances at high latitudes (Yoon and Chen 2006). The climate system of eastern Siberia is a unique and interactive land-atmosphere system.

Snow cover in eastern Siberia plays a critical role in land-atmosphere climate system. Matsumura et al. (2010) investigated the effect of anomalous springtime snow cover in northern Eurasia on the summertime land-atmosphere climate system using an atmospheric general circulation model (AGCM). On the basis of the modeling study, Matsumura and Yamazaki (2012) examined the land-atmosphere climate system employing observation and reanalysis data. Figure 1 shows a schematic of seasonal changes in early-snowmelt years from winter to autumn in eastern Siberia. Because the ground conditions are sufficiently dry to enable the storage of snowmelt water within the soil, the snow-hydrological effect (e.g., Yasunari et al. 1991) is prominent during summertime; that is, enhanced soil moisture (snowmelt water) persist later into the summer, contributing to surface cooling and a coupling between evaporation and precipitation (precipitation recycling) (e.g., Numaguti 1999). Similarly, less snow cover in spring results in reduced snowmelt water and correspondingly lower soil moisture in summer (higher surface air temperature), resulting in reduced cloudiness, evaporation, and precipitation (higher surface air temperature). Consequently, the snow-hydrological effect and precipitation recycling maintain the surface heating or cooling during summer in eastern Siberia. This climate memory of soil moisture can persist for a few months (Delworth and Manabe 1989; however, just atmospheric forcings cannot persist.

Because of surface heating through the climate memory effect, in late summer, tropospheric heating is caused by condensation heating associated with ascending air masses and adiabatic heating of descending air masses, forming a stronger upper-level anticyclone with a westward tilt. Because the upper-level anticyclone with a baroclinic structure is located to the west of the Sea of Okhotsk, Matsumura and Yamazaki (2012) suggested that this anticyclone may play a dominant role in the development of the surface Okhotsk High (OH) in late summer.

The frequent occurrence of the summer OH, which is a quasi-stationary surface high-pressure system during the warm season from late April to early September, often leads to abnormally cool summers in northern Japan due to the cool and wet surface northeasterly over cool sea surface, especially in July and August (e.g., Ninomiya and Mizuno 1985a; Ninomiya and Mizuno 1985b). Understanding OH is important for seasonal forecasts of summertime weather in northeastern Asia; however, it remains difficult to predict its development because of the complex interactions between atmospheric, oceanic, and land

surface processes. In addition, tropical forcing (e.g., the Pacific-Japan (PJ) teleconnection pattern) (Nitta 1987) influences the variability of the OH (Wakabayashi and Kawamura 2004). The formation mechanism of the OH in early summer has been described in terms of atmospheric dynamical processes (Nakamura and Fukamachi 2004; Sato and Takahashi 2007), whereas its mechanism in late summer remains unclear.

The present study is mainly based on the results of Matsumura et al. (2010) and Matsumura and Yamazaki (2012), and attempts to make a connection between springtime snow cover and development of the late summer OH. To clarify the role of spring snow cover in Siberia on summer OH, atmospheric circulation outside the Siberia- Okhotsk region should be prescribed for years when OH developed because OH does not necessarily develop every year. Therefore, using a regional climate model (RCM) is useful for understanding the relationship between snow cover and the quasi-stationary OH in terms of land-atmosphere climate system. Fischer et al. (2007) performed sensitivity simulations using an RCM and demonstrated that soil moisture anomalies had a substantial impact on the strength of the 2003 European summer heat-wave and affected the extent of anticyclonic anomalies. Thus, using an RCM is highly effective for reproducing the intensively developed quasi-stationary OH in typical years.

The remainder of this paper is organized as follows. Section 2 describes interannual variation of the OH and discusses the seasonality of the formation mechanism of the OH. Section 3 presents the land-atmosphere coupling in eastern Siberia and development of the August OH in typical years. Finally, a discussion of the results and the main conclusions are given in Sections 4 and 5, respectively.

2. Seasonal variation of the OH structure

First, we describe the characteristic of the August OH as well as the difference between the early and late summer OH. We perform a regression analysis defined by an August OH index (area-averaged 1000-hPa geopotential height within the region 50–60°N, 140–155°E), as shown in Fig. 2a, using the National Centers for Environmental Prediction Department of Energy Atmospheric Model Intercomparison Project reanalysis (NCEP2) (Kanamitsu et al. 2002), which is similar to the approach of Tachibana et al. (2004), although they only focused on July. The August OH index has a downward trend when long-term trend is not removed (not shown). Figure 2a shows the monthly mean 1000-hPa geopotential height, which is linearly regressed onto the detrended OH index from 1979 to 2012. Although the Sea of Okhotsk is usually covered by dense fog in summer, the reanalysis data are unable to reproduce fog with cold boundary layer air masses, which may deform the lower levels over the Sea of Okhotsk (Tachibana et al. 2004). Nevertheless, the results obtained using 850-hPa geopotential height as the OH index are similar to those obtained using 1000-hPa geopotential height.

Upper-level anticyclonic anomalies clearly form over eastern Siberia (Fig. 2b), located to the west of the center of the OH (Fig. 2a), and extend northward to the Arctic coast and westward to the inland area. Figures 2c and d show vertical cross sections of the geopotential height and air temperature along 55°N, respectively. Geopotential height anomalies exhibit a westward tilt with height, and significant positive air-temperature anomalies are found between the surface and the upper troposphere over eastern Siberia, reflecting a distinct baroclinic structure throughout the entire troposphere. Consequently, the OH develops with a distinct baroclinic structure in eastern Siberia, suggesting that land surface forcing can contribute to the amplification and maintenance of the baroclinic structure.

Furthermore, eastern Siberia is more suitable for the development of the stationary waves in August as well as early autumn (Cohen et al. 2007) when snow cover increases. Figure 3a shows climatological 300-hPa zonal wind (shadings) and wind vectors in August for the period 1979–2012. The upper troposphere over eastern Siberia exhibits an anticyclonic circulation, while over western Siberia it exhibits a cyclonic circulation, indicating that the upper troposphere over northern Eurasia is dominated by the wavy structure. In addition, because eastern Siberia is located near the subpolar jet (Fig. 3b), the lower troposphere with a baroclinic response because of surface heating favors the upward propagation of wave activity, especially in early snowmelt years (Matsumura and Yamazaki 2012). These results suggest that land surface forcing in eastern Siberia can act to reinforce and maintain the baroclinic structure, resulting in the August OH development.

Nakamura and Fukamachi (2004) reported that the OH development in early summer is caused by interaction between a stationary Rossby wave packet and surface baroclinicity (nearly equivalent barotropic structure). Moreover, we examined the seasonality of the summer OH in terms of interannual variations using the same analysis linearly regressed onto the

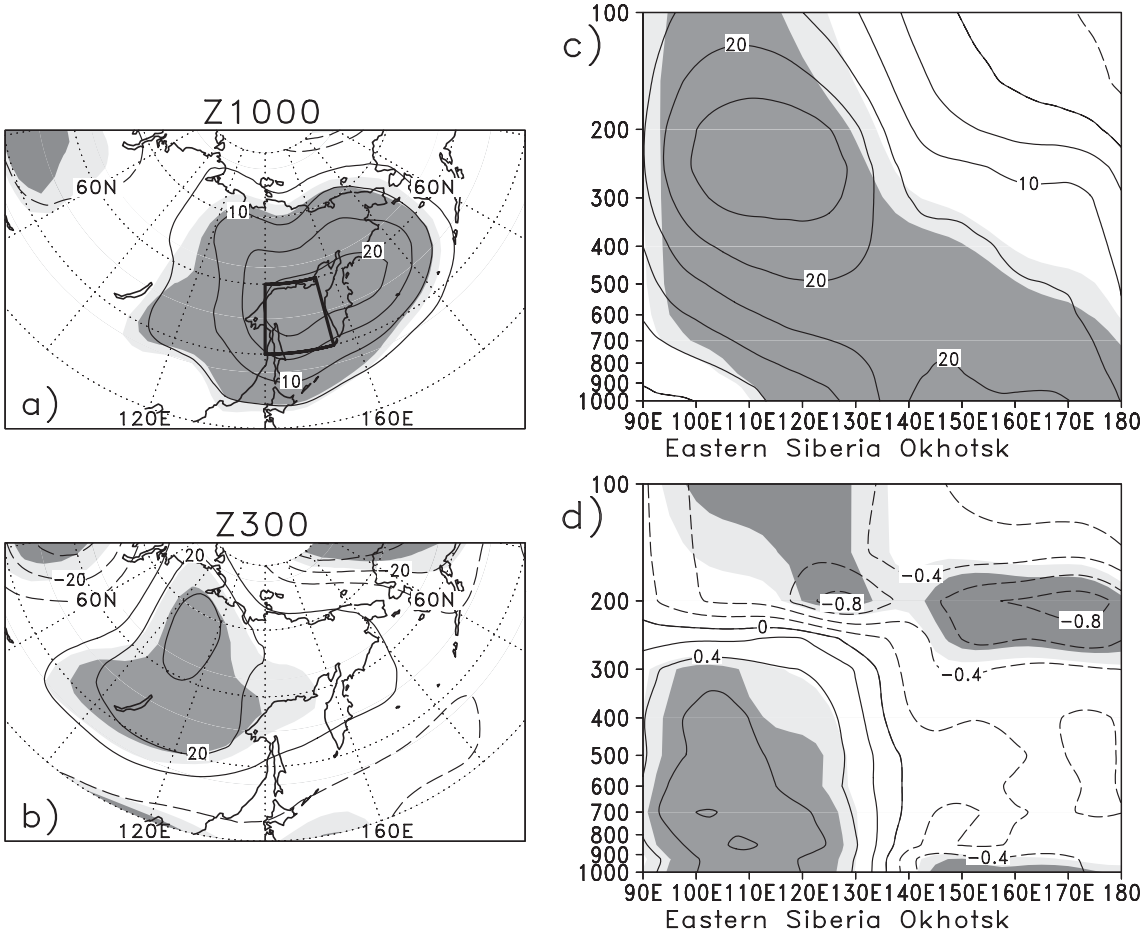

Fig. 2. Monthly atmospheric patterns linearly regressed onto the Okhotsk high index (regions surrounded by thick solid lines: 50–60°N, 140–155°E) in (a) 1000-hPa geopotential height (5 m contour interval) and (b) 300-hPa height (10 m contour interval) based on the NCEP2 reanalysis in August during 1979–2012. (c) Longitude-pressure sections of height (5 m contour interval) and (d) air temperature (0.2 K contour interval) along 55°N. Light and heavy shadings indicate statistical significance at the 95 % and 99 % levels, respectively.

June and July OH index (Figs. 4a, d). In June, upper-level anticyclonic anomalies clearly form over and around the Sea of Okhotsk (Fig. 4b), which account for an equivalent barotropic structure throughout the entire troposphere (Fig. 4c), even though the anomalies exhibit a slight northward tilt with height. In July, geopotential height anomalies exhibit a northwestward tilt with height (Fig. 4e) as well as a surface baroclinicity (Fig. 4f), indicating a nearly equivalent barotropic structure. Consequently, the formation mechanism of the surface high clearly differs between early and late summer because the August OH develops with a baroclinic structure throughout the entire troposphere over eastern Siberia. In June, significant upper-level anticyclonic anomalies reach only below the near-tropopause (approximately 250-hPa), in July above the tropopause, and in August the highest in summer (Fig. 2c). In September, when soil surface begins to freeze in northern Eurasia, geopotential height anomalies exhibit an equivalent barotropic structure in the troposphere over around the Sea of Okhotsk (not shown), suggesting a weakening of baroclinic structure. Consequently, the OH changes from an equivalent barotropic to a baroclinic structure with seasonal changes during the warm season.

In addition, climatological upper westerlies differ between early and late summer. Following strong land-sea surface temperature contrast across the Arctic coast, the subpolar jet becomes apparent over around

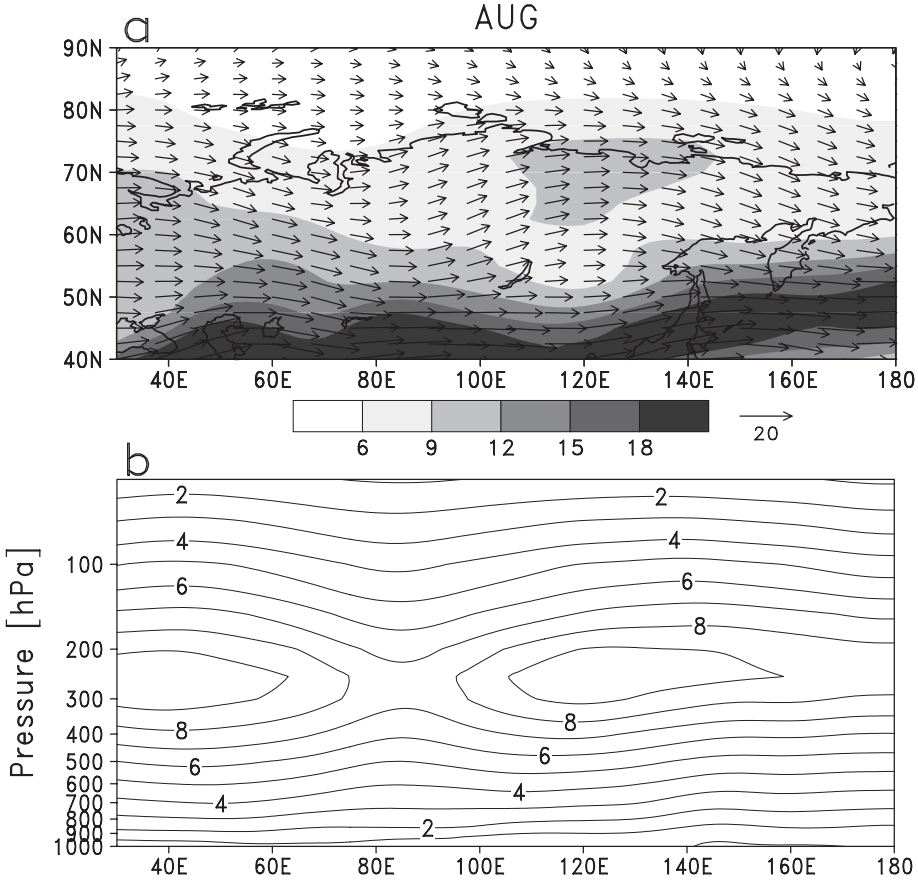

Fig. 3. (a) Climatological 300-hPa zonal wind (shaded; m s^{-1}) and vector (arrows; m s^{-1}), and (b) longitude-pressure sections of zonal wind (1 m s^{-1} contour interval) averaged the areas of 60–70°N in August for the period 1979–2012.

the northeastern Siberia (north of 60°N) in June, whereas over the Sea of Okhotsk westerlies weaken and form a double-jet structure (Fig. 5a). Northeastern Siberia is located near the subpolar jet (Fig. 5b), suggesting that the upper troposphere favors wave propagation from the west. In July, when the land-sea temperature contrast across the Arctic coast is the strongest, the subpolar jet clearly forms along the Arctic coast, and the westerlies weaken along approximately 60°N over the northern Eurasia (Fig. 5c), indicating that the westerlies are roughly distributed in the zonal direction over northern Eurasia (Figs. 5c, d). Thus, the upper troposphere over northern Eurasia favors wave propagation from the west. Indeed, a stationary Rossby wave along the Arctic coast contributes to the formation of an upper-level ridge over the OH in July (Nakamura and Fukamachi 2004). These results suggest that eastern Siberia can be a Rossby wave source in August, while in June and July, the upper troposphere is influenced by wave propagation from the west, which accounts for the different formation mechanism of the OH between early and late summer.

3. RCM experiments

3.1 Typical year of the August OH

In the previous section, we examined seasonal variation of the OH using the monthly OH index. However, the OH is a quasi-stationary surface high-pressure system instead of a stationary system, especially significant in late summer due to its baroclinicity. As noted earlier, the formation mechanism of the OH in early summer has been well described in many studies, whereas its mechanism in late summer remains unclear. Moreover, the August OH has not been clearly defined as compared to the most developing early summer OH. However, it has been suggested that in the late August of 2008 the

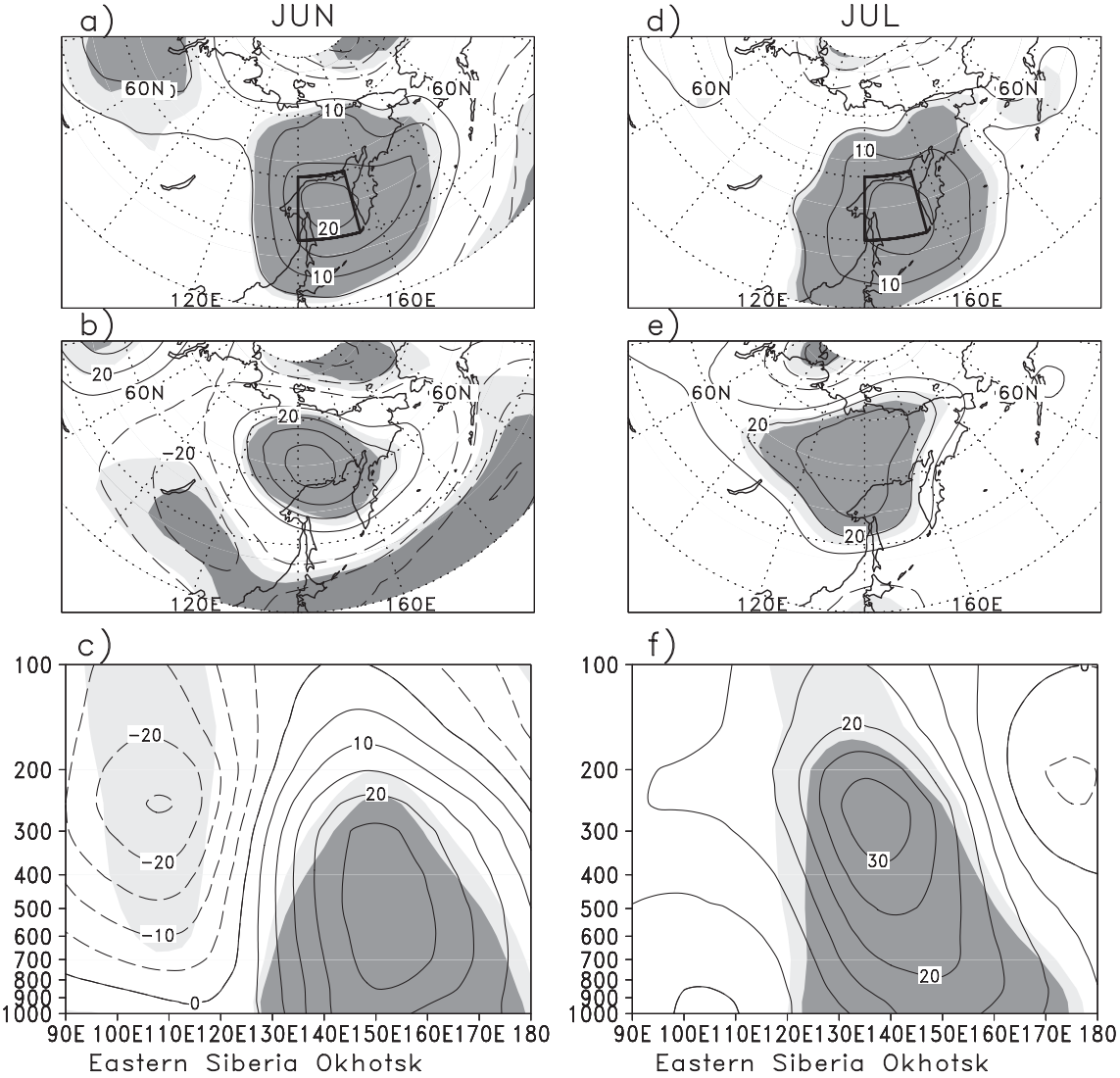

Fig. 4. As in Figs. 2a, 2b, and 2c, but for June and July.

quasi-stationary surface high-pressure system around the Sea Okhotsk contributes to heavy rainfall over Japan (Japan Meteorological Agency 2008). Therefore, we attempt to understand the development of the surface high-pressure system as the August OH using an RCM. Because the August OH does not necessarily develop every year, we perform RCM experiments in 2008, when the August OH index is the highest in recent decades, and additional experiments in 2002, when the August index is the highest in the past few decades.

Prior to performing RCM experiments, we will show the quasi-stationary surface high-pressure system around the Sea of Okhotsk in late August 2008 as a typical scenario. Figure 6a shows sea-level pressure (SLP), 10-m wind, and 300-hPa geopotential height during 16–28 August 2008 based on the NCEP2 reanalysis. The surface anticyclone over the Sea of Okhotsk intensively develops with a baroclinic structure and extends southeastward toward northern Japan. Because the center of the anticyclone is located over the southern Sea of Okhotsk, the surface north-easterlies over cool ocean causes lower temperatures over northern Japan. These results indicate that the quasi-stationary surface high-pressure system in late August of 2008 has a common characteristic similar to the OH. In eastern Siberia, on the other hand, higher surface temperatures are observed (Fig. 6b), and early snowmelt is seen (Fig. 6c).

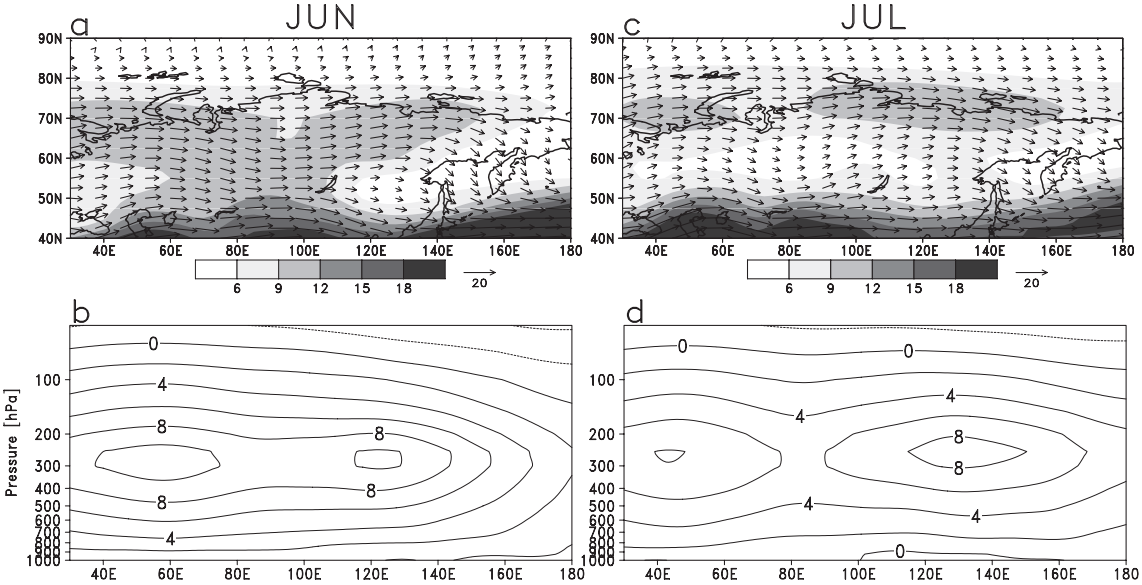

Fig. 5. As in Fig. 3, but for June and July.

Therefore, we attempt to make a connection between springtime snow cover and the development of the August OH in 2008 using the same approach as the AGCM experiments of Matsumura et al. (2010) to isolate the impact of snow anomaly.

3.2 Experimental design

We used the Weather Research and Forecasting (WRF) model version 3 with the Advanced Research WRF (ARW) dynamic core (Skamarock et al. 2008), which is based on compressible nonhydrostatic equations. The numerical simulation domain is the area shown in Fig. 6, which is divided into 180130 grid points with a horizontal resolution of 30 km and 28 vertical levels. The model uses the Yonsei University planetary boundary layer scheme (Hong et al. 2006); the Kain-Fritsch cumulus parameterization (Kain 2004), representing the effects of convection on subgrid scales; the WRF single moment 3-class microphysical scheme (Hong et al. 2004); the Rapid Radiative Transfer Model (RRTM) for longwave parameterization (Mlawer et al. 1997); and the Dudhia scheme for shortwave radiation (Dudhia 1989). The land surface model (LSM) used in this study is Noah LSM (Chen and Dudhia 2001), which is a 4-layer (0–10, 10–40, 40–100, and 100–200 cm) soil temperature and moisture model with fractional snow cover and soil ice prediction.

The results of two experiments with initial snow mass anomalies are compared to examine the influence of springtime snow cover on the summer OH development. The 6-hourly data of the NCEP2 reanalysis are used as the initial and lateral boundary conditions. Model integration was conducted from 1 May to the end of September 2008 with the prescribed sea surface temperature (OISST) (Reynolds et al. 2002) for the control run (CTL run). For the heavy-snow run (SNOW run), we prescribed an initial snow mass (water equivalent) in the snow-covered region of the Eurasian continent obtained from the reanalysis data on 1 May, which is three times (× 3) than that in the CTL run, using the same approach as the AGCM experiments of Matsumura et al. (2010). We note that the initial soil moisture is the same conditions in both the CTL and SNOW runs. For stochastic manners in an RCM experiment, the differences between atmospheric initial conditions can be neglected, as compared to the interannual variations (Fischer et al. 2007) because RCM is forced by lateral boundary data. Under the same model configuration except for the initial snow mass, we performed additional experiments for the SNOW run, and obtained roughly similar results.

3.3 Land-atmosphere coupling in eastern Siberia

We reproduced the land-atmosphere coupling in eastern Siberia. Figure 7 shows time variation of 11-day low-pass-filtered surface parameters averaged over the eastern Siberia in the CTL and SNOW runs. The simulated surface air temperatures are consid-

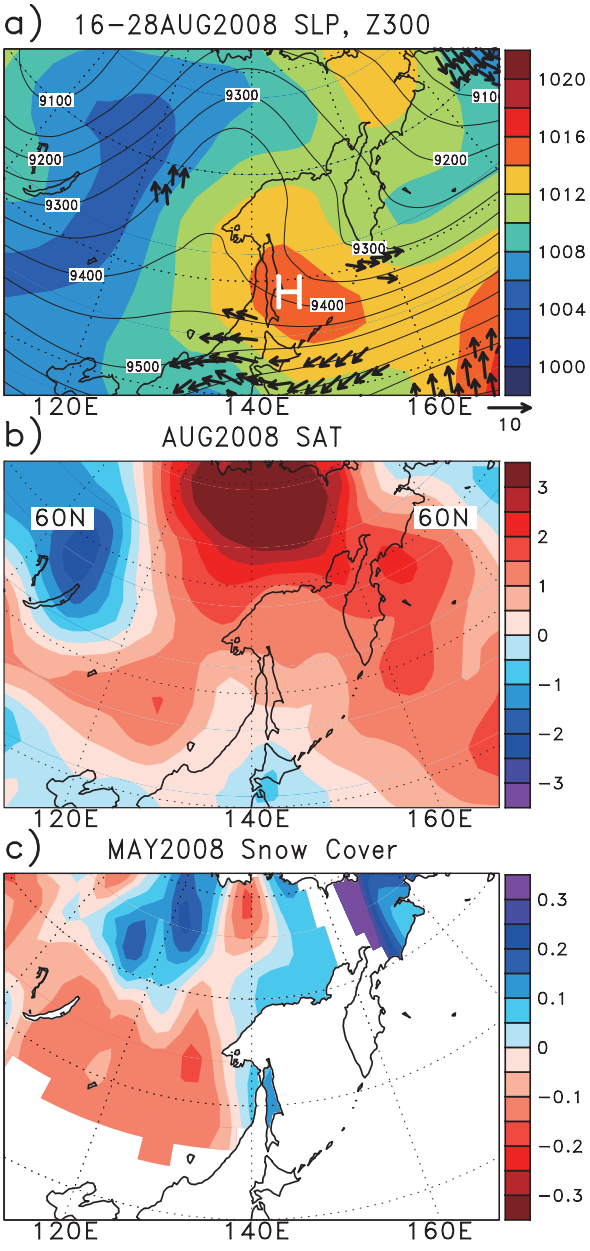

Fig. 6. (a) Typical weather pattern developed in August OH for the period 16–28 August 2008 based on the NCEP2 reanalysis, showing mean sea-level pressure (shadings; hPa), 10-m wind (arrows; m s^{-1}), and 300-hPa geopotential height (50 m contour interval). (b) Surface air temperature anomalies (°C) in August 2008 based on the NCEP2 reanalysis. (c) Observed snow cover ratio anomalies in May 2008 based on station data (Yabuki et al. 2011).

erably well consistent with the variations observed at Olekminsk (60°N, 120°E). The result of the CTL run is similar to the observed temperature variations than the result of the SNOW run, except for June. As described by Matsumura et al. (2010), the less snow mass in the CTL run results in increased solar radiation and reduced snowmelt energy, which accounts for the increase in surface heating during the melting period. The CTL run underestimates the temperature in May that may have resulted from the NCEP2 reanalysis as the initial snow mass and soil moisture. The difference in initial snow mass between the two runs results in a large difference in surface soil moisture in May.

In June, the observed temperature is more similar to the SNOW run because of the increased cumulus precipitation in the CTL run. Cumulus precipitation contributes to the total precipitation differences (bottom figure), resulting in decreased temperature due to increased cloudiness. After July, the total precipitation shows a greater increase in the SNOW run than in the CTL run, reflecting the increased soil moisture and decreased surface air temperature. The surface air temperatures in August are significantly higher in the CTL run than in the SNOW run. After July, the large-scale precipitation dominantly contributes to total precipitation differences between the CTL and SNOW runs. In addition to ground condition, atmospheric conditions are also significantly dry over eastern Siberia, where recycled water is a major source of precipitation (e.g., Numaguti 1999). Thus, the precipitation differences reflect initial anomalous snow mass. After September, the surface air temperatures in the CTL run are in good agreement with those in the SNOW runs, but there are considerable differences between the two runs and observed temperature variations. This indicates that surface climate memory of soil moisture (herein anomalous initia l snow mass) persists for only a few months (e.g., Walsh et al. 1985; Delworth and Manabe 1989).

Further, influence of the land-atmosphere coupling appears in deeper soil layers. Figure 8a shows the time-depth sections of differences in soil temperature and moisture. After September, in deeper soil layers soil moisture differences are enhanced with the thawing of the frozen soil because of the decreased precipitation in the CTL run after July. However, there is little increased soil-thawing water in deeper soil layers because thawing of the frozen soil reaches the lowest layer by the end of August.

Prior to July, on the other hand, surface soil moisture differences decrease as a result of infiltration of

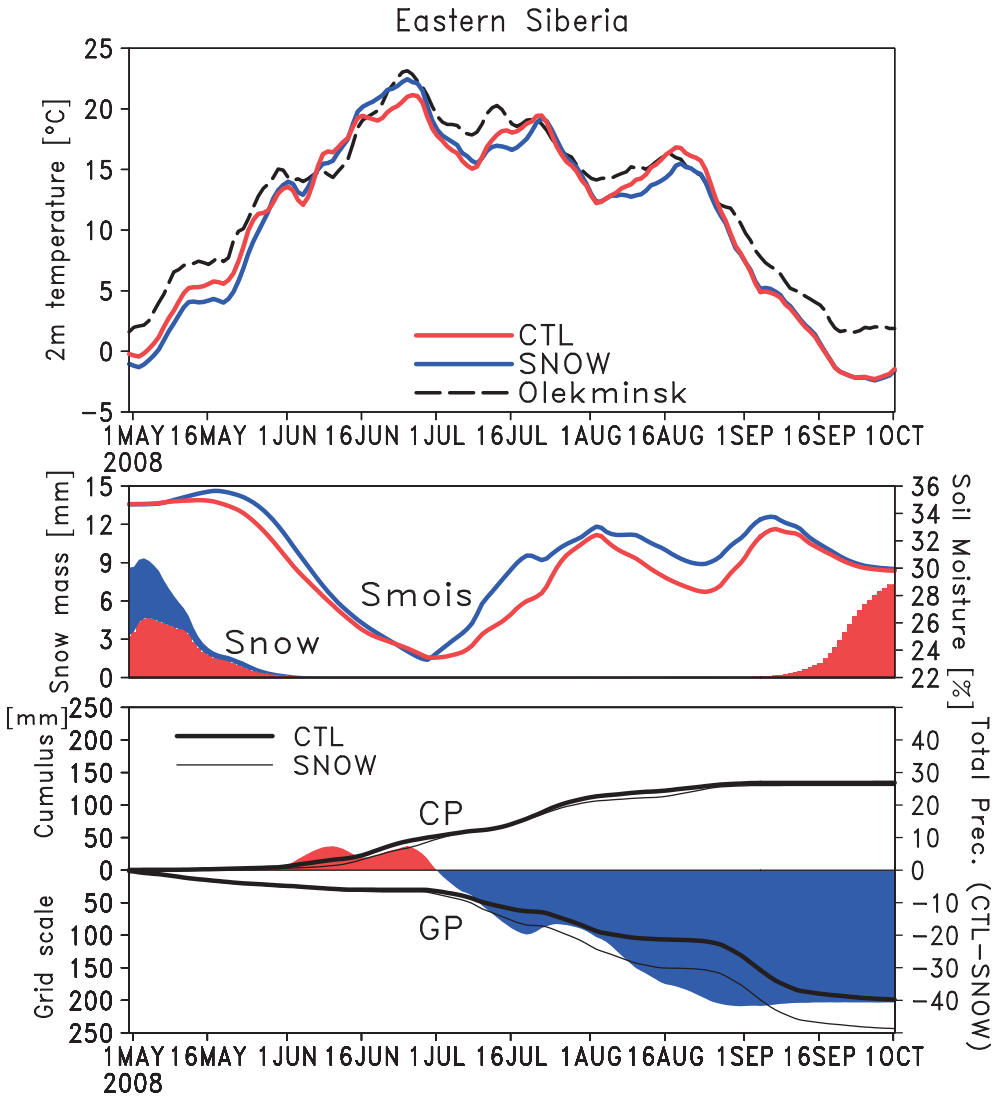

Fig. 7. Time series of 11-day low-pass-filtered surface parameters averaged over eastern Siberia (60°N, 120–130°E) in the CTL (red shadings and lines) and SNOW (blue shadings and lines) runs from May through September in 2008. Top panel: 2-m air temperature (°C) and observed surface air temperature (dashed line) at Olekminsk (60°N, 120°E) based on station data. Middle panel: snow mass (shadings; mm) and 10–40 cm soil moisture (%). Lower panel: accumulated cumulus precipitation (CP), sub-grid scale precipitation (GP), and total precipitation differences (shadings) between the CTL and SNOW runs.

snowmelt water (Fig. 8a), while soil liquid water increases with thawing of the frozen soil in the CTL run (Fig. 8b) because of early thawing of the frozen soil. Increased soil water in the shallow soil layer might contribute to increase June cumulus precipitation in the CTL run because of local precipitation recycling. Indeed, latent heat flux in the CTL run is slightly larger than that in the SNOW run (Fig. 8c). However, AGCM experiments of Matsumura et al. (2010) do not capture the increased June convective precipitation, which possibly depends on the cumulus parameterization or model resolution. After July, when the soil thawing reaches in deeper soil layers, however, there is little soil-thawing water difference because of little soil temperature difference in deeper soil layers. Consequently, soil moisture and water rapidly decrease in the CTL run and reaches a maximum in September. Corresponding to the

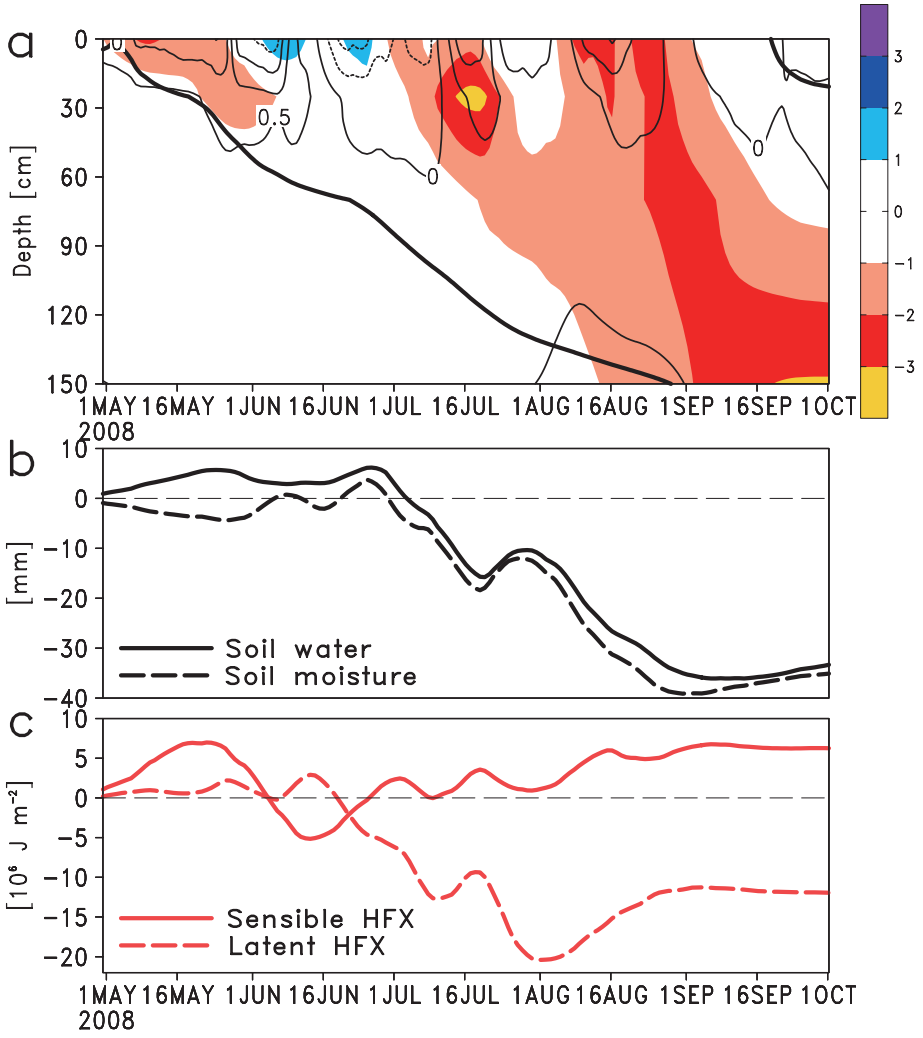

Fig. 8. As in Fig. 7, but for (a) time-depth sections of the CTL – SNOW differences in soil temperature (0.5°C contour interval) and moisture (shadings; %), and (b) time series of the CTL – SNOW differences in vertically accumulated soil moisture (dashed line) and liquid water (solid line) and (c) accumulated upward surface sensible (solid line) and latent (dashed line) heat fluxes. The bold solid contours in (a) indicate 0°C in the CTL run.

decreased soil water, latent heat flux differences also change its sign, which implies that the evaporation in the CTL run decreases compared with that in the SNOW run. Because evaporation efficiency decreases with decreasing soil wetness, the evaporation in the CTL run becomes much smaller than that in the SNOW run. To balance the decreased latent heat flux, sensible heat flux increases after July. Consequently, the decreased evaporation contributes to the decreased precipitaion, which further contributes to maintain the drier soil moisture conditions and warmer surface temperature, leading to the land-atmosphere coupling in late summer.

In conclusion, reduced springtime snow cover results in less snowmelt water and correspondingly lower soil moisture, resulting in turn in reduced evaporation and precipitation after July. These are consistent with the results of Matsumura et al. (2010)'s AGCM experiments, and support that the combination of the snow-hydrological effect and coupling between evaporation and precipitation leads to anomalous surface heating or cooling in eastern Siberia.

3.4 Development of the August OH

To examine the atmospheric response to anomalous snow cover, we focus on the period of lasted surface

heating (9–28 August in Fig. 7). Figure 9a shows SLP, 10-m wind, and 300-hPa geopotential height during the first half (9–15 August) of the period in the CTL run. Significant OH is not developed in the CTL run. However, the SLP differences between the CTL and SNOW runs (CTL minus SNOW) are clearly appeared over the southern Sea of Okhotsk (contours in Fig. 9b). The lower surface temperatures in the CTL run are because of the cool surface north-easterlies over the cool sea surface of the Sea of Okhotsk, while in eastern Siberia, higher surface temperatures appear, as shown in Fig. 7. The 850-hPa height differences are also enhanced over the southern Sea of Okhotsk and eastern Siberia (Fig. 9c). In the upper troposphere, however, strong anticyclonic differences develop over eastern Siberia, whereas cyclonic differences form over the Sea of Okhotsk (Fig. 9d). These results indicate that the intensified SLP over the Sea of Okhotsk develops with a distinct baroclinic structure due to initial anomalous snow mass.

Figure 10a shows the August OH during the second half (16–28 August) of the period of lasted surface heating. The CTL run well reproduces the observed OH (Fig. 6a). The OH extends southeastward to near northern Japan, forming a baroclinic structure, which is similar to the observed OH. The intensified OH is clearly appeared over the Sea of Okhotsk (contours in Fig. 10b). In addition, another intensified SLP is located to the east of the Kamchatka Peninsula, suggesting that it was formed during the first half of the period. Although in eastern Siberia positive temperature anomalies may be caused by not only thermal heating but also the intensified OH, higher surface temperature last, whereas in the Sea of Okhotsk and northern Japan lower surface temperatures last (shadings in Fig. 10b), strengthening the land-sea thermal contrast. The 850-hPa height differences are also enhanced over the Sea of Okhotsk and eastern Siberia, extending southeastward to near northern Japan (Fig. 10c). In the upper troposphere, strong anticyclonic differences develop over eastern Siberia, whereas cyclonic differences form around the Sea of Okhotsk (Fig. 10d). These results suggest that land-atmosphere coupling in eastern Siberia contributes to the development of the August OH with a distinct baroclinic structure.

Now, we will show the vertical cross-sections of differences in geopotential height, air temperature, and vertical velocity averaged for the area 50–60°N between the CTL and SNOW runs during the first and second half of the period, as shown in Fig. 11. In the first half of the period, strong anticyclonic differences exhibit a westward tilt with height over eastern Siberia and the Sea of Okhotsk. Enhanced ascent appears over eastern Siberia and significantly enhanced descent appears over the Okhotsk Sea between the surface and the upper troposphere. Because of surface heating through the snow-hydrological effect, in late summer, tropospheric heating is caused by condensation heating associated with ascending air masses and adiabatic heating of descending air masses, forming a stronger upper-level anticyclone with a baroclinic structure (Matsumura and Yamazaki 2012). In the second half of the period, the strong anticyclonic differences extend eastward, weakening its baroclinicity. However, enhanced descent remains over the Okhotsk Sea, resulting in surface anticyclonic differences called "the Okhotsk High" in this area. Consequently, the regional land-atmosphere coupling can help to reinforce and maintain the baroclinic structure through surface heating over eastern Siberia, forming strong surface anticyclone.

3.5 August OH in 2002

To further confirm the formation mechanism of the August OH, we also performed additional sensitivity experiments in 2002, when the August OH index is the second highest year since 1979. Figure 12a shows SLP, 10-m wind, and 300-hPa geopotential height for the period of lasted surface heating over eastern Siberia 13–27 August 2002 in the CTL run. The CTL run well reproduces the August OH in 2002 (not shown), although the OH tends to develop significantly over the Sea of Okhotsk. The OH extends northeastward to the Kamchatka Peninsula, causing surface north-easterlies. The upper-level ridge is located over eastern Siberia, forming a baroclinic structure. Figure 12b shows differences in surface air temperature, SLP, and 10-m wind between the CTL and SNOW runs. Higher surface temperatures appear in eastern Siberia, whereas lower surface temperatures appear in Mongolia and northern China (shadings), resulting in the north-south contrasting responses across 50°N. The lower surface temperatures are mainly due to north-easterlies and increased cloudiness. This is because of the strengthening of the OH-like response in the CTL run (contours), even though the center of the intensified SLP is not located over the Sea of Okhotsk. The intensified OH-like response appears to extend east-southeastward to near northern Japan. The 850-hPa height differences are also enhanced over southeastern Siberia, extending southeastward to the Sea of Okhotsk (Fig. 12c). In the upper troposphere, however, strong anticyclonic

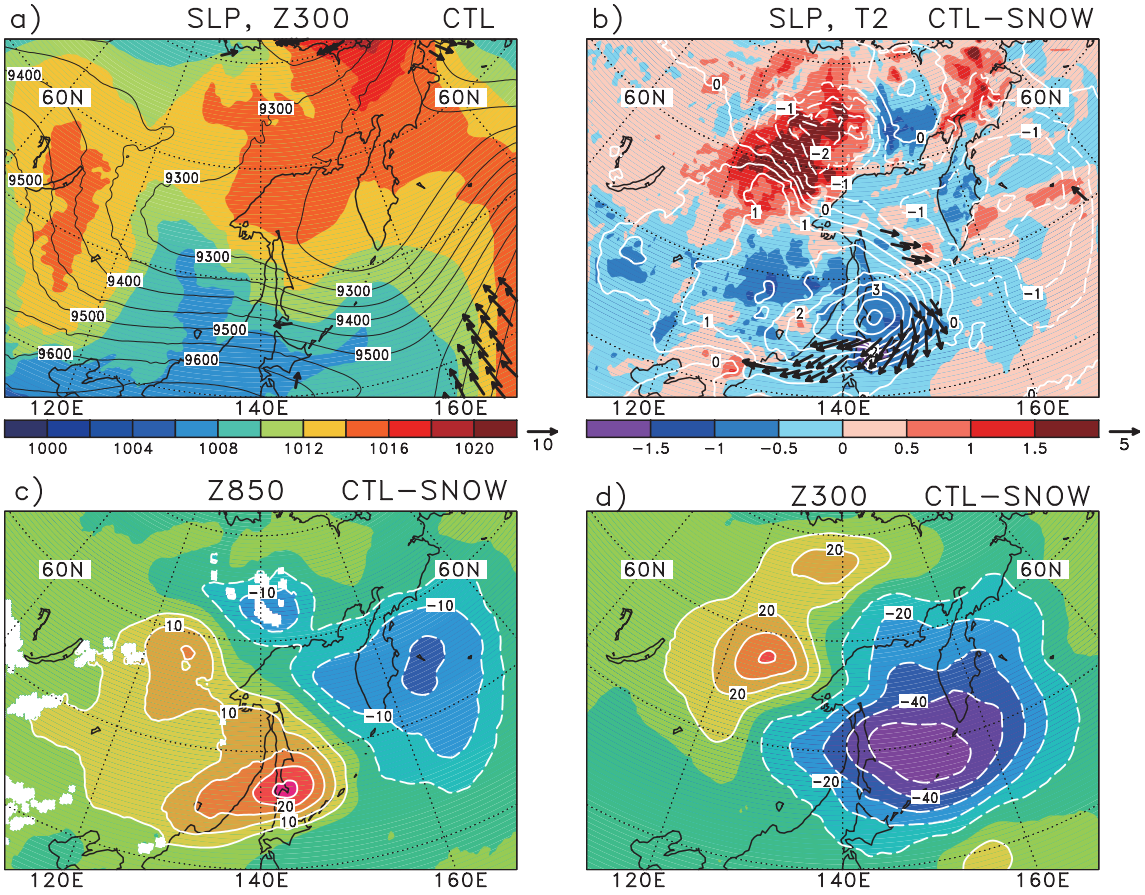

Fig. 9. (a) Distribution of sea-level pressure (shadings; hPa), 10-m wind (arrows; m s^{-1}) and 300-hPa geopotential height (50 m contour interval) for the period 9–15 August 2008 in the CTL run. (b) Differences in 2-m air temperature (shadings; °C), SLP (0.5 hPa contour interval), 10-m wind (arrows; m s^{-1}), (c) 850-hPa and (d) 300-hPa geopotential height between the CTL and SNOW runs.

differences develop over eastern Siberia, whereas cyclonic differences form over the Okhotsk Sea and northern China (Fig. 12d), forming a baroclinic structure. These results also support that land-atmosphere coupling in eastern Siberia can help to reinforce and maintain the baroclinic structure.

4. Discussion

4.1 Role of snow cover in the seasonal evolution of the OH

What is the meaning of the different formation mechanism of the OH between early and late summer? In early summer, stationary Rossby waves contribute to the formation of an upper-level ridge over around Sea of Okhotsk, forming the surface OH because of a nearly equivalent barotropic structure (Nakamura and Fukamachi 2004). Our experimental results of July OH 2008 also indicate that geopotential height over the Sea of Okhotsk simulated by the CTL run strengthens than that of the SNOW run in the entire layer of the atmosphere (not shown), which account for a nearly equivalent barotropic structure throughout the entire troposphere. In August, on the other hand, the regional land-atmosphere coupling can contribute to the amplification and maintenance of the baroclinic structure through surface heating over eastern Siberia, forming strong anticyclone with a baroclinic structure.

Observations only capture one realization of many possible climate variations, and include both atmospheric internal variability and anomalies forced by slowly varying surface boundary conditions such as snow cover and soil moisture in northern Eurasia. The atmospheric internal variability also contributes to the

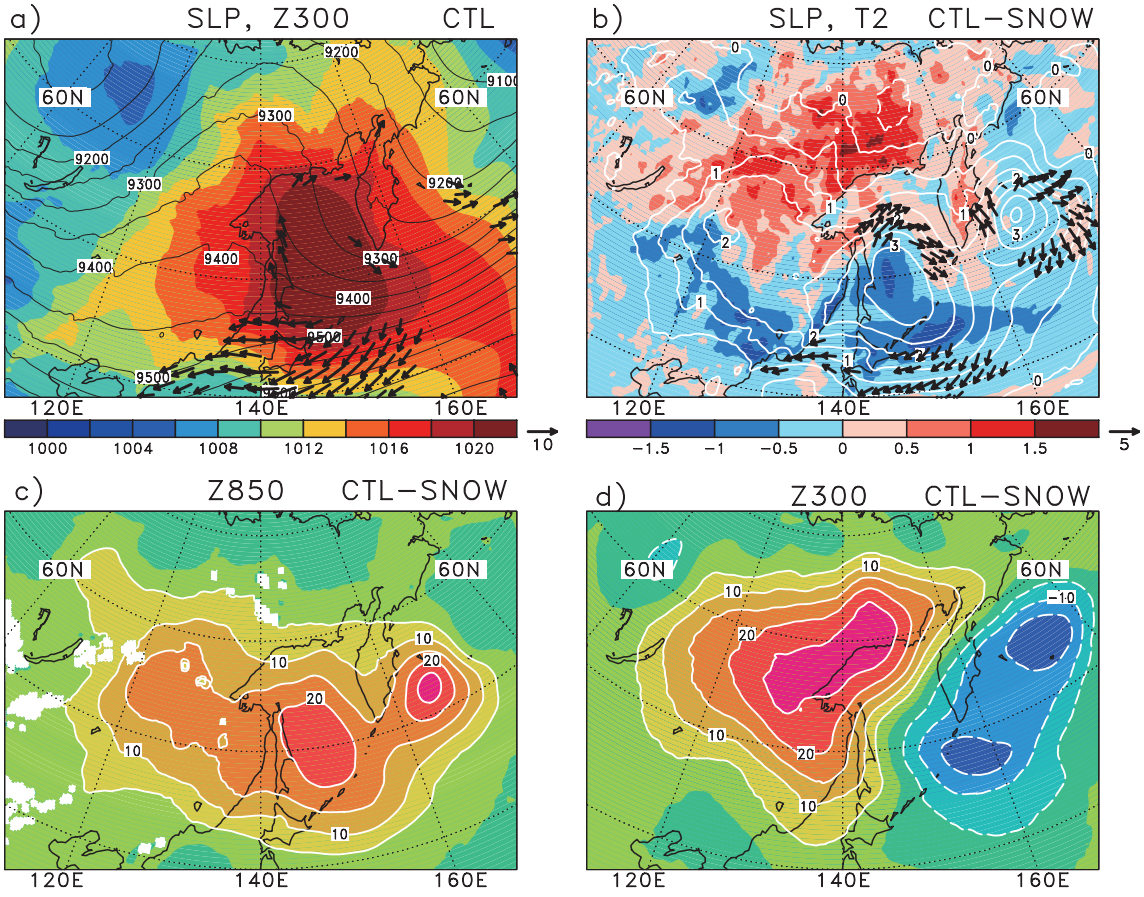

Fig. 10. As in Fig. 9, but for the period 16–28 August 2008.

development of the OH because blocking formation leads to the development of the OH in early summer, as shown by many previous studies. Seasonal evolution of the land surface warming accompanied with snowmelt in northern Eurasia leads to the land-sea temperature contrast across the Arctic coast, which may help to determine a favorable environment for the occurrence and maintenance of blocking. Indeed, snow cover and land surface temperature anomalies can modulate regional blocking activity (Arai and Kimoto 2005; Garcia-Herrera and Barriopedro 2006). However, changes in snow cover solely cannot account for the interannual variations in the OH because tropical forcing such as PJ pattern has a significant influence on the variability of the OH (Wakabayashi and Kawamura 2004). Indeed, our regression analysis indicates that the PJ-like pattern corresponds to the OH index, especially in the mid-troposphere (not shown).

4.2 Role of rainfall and frozen soil in land-atmosphere coupling

For the land-atmosphere climate system, it is important to better understand the role of individual processes, i.e., not only snow cover but also rainfall and frozen soil. Rainfall processes over eastern Siberia are different in early and late summer under anomalous initial snow conditions. Yamada (2007) demonstrated that the influence of land surface moisture conditions on convective rain cannot be ignored; they simulated rainfall over the Tibetan plateau and showed that dry elevated surface is favorable for more convective rain whereas wet surface condition is favorable for stratiform cloud but with more rainfall, which is similar to our results. Dry ground conditions in eastern Siberia are very similar to the elevated region, reflecting light snow (dry) and heavy snow (wet) conditions. In early summer, surface heating under dry conditions (CTL run) leads to increased cumulus precipitation, resulting in turn in

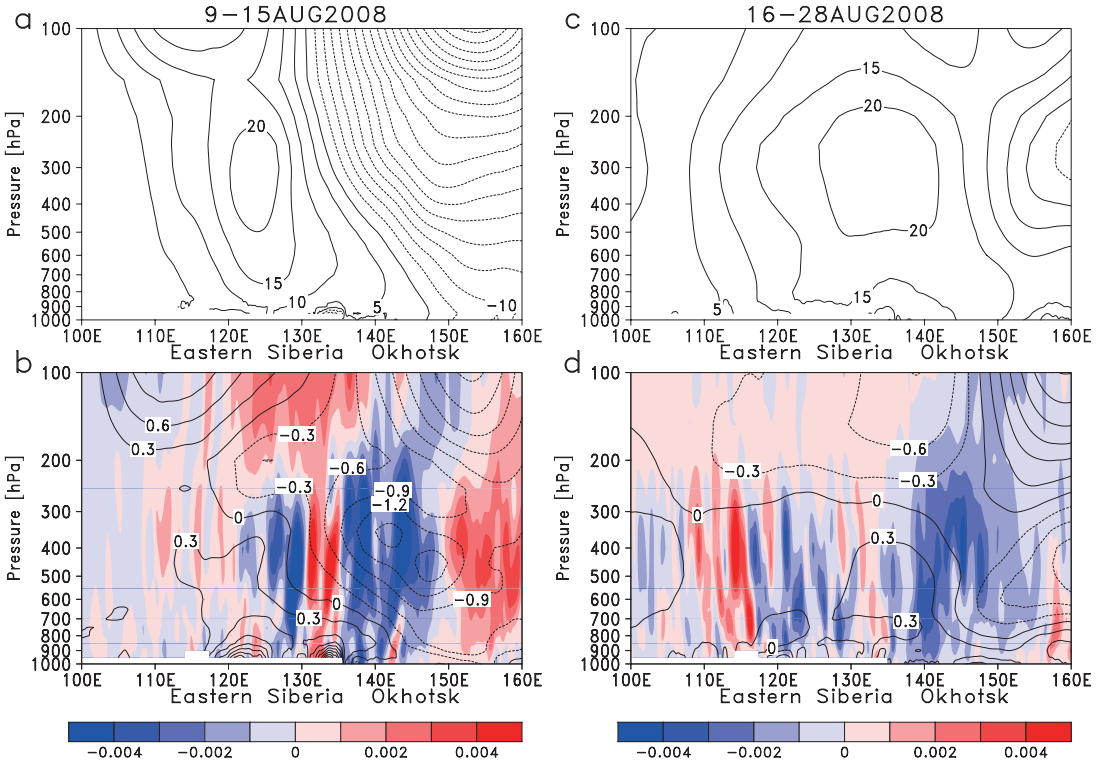

Fig. 11. Longitude-pressure sections of differences in (a) geopotential height (5 m contour interval), (b) air temperature (0.3 K contour interval) and vertical velocity (shadings; m s^{-1}) (positive values indicate upward) between the CTL and SNOW runs during 9–15 August 2008 averaged the areas of 50–60°N. (c) and (d): As for (a) and (b), but for during 16–28 August 2008.

lower surface air temperature due to increased cloud cover. In late summer, on the other hand, wet conditions (SNOW run) lead to increased evaporation and grid scale precipitation, resulting in lower surface air temperature. Therefore, it is necessary for the better understanding of the rainfall processes to use a higher resolution RCM so that it can resolve convective rainfall in dry ground conditions.

The impermeability of frozen soil to spring meltwater leads to increased runoff; consequently, summer soil wetness is significantly reduced, resulting in turn in an increase in summertime surface temperatures over boreal continents (Takata and Kimoto 2000). Furthermore, we did not consider the insulating effect of snow cover from the time of snow-appearance to the melting period. A thicker snow cover would prevent the ground from cooling, whereas a thinner snow cover would enable heat transfer from the atmosphere. Consequently, snow mass affects the frozen soil temperature, snowmelt water within the soil, and the resulting snow-hydrological effect. It is possible that the reproducibility of RCM in eastern Siberia during autumn depends on the land surface processes such as the timing of snow-appearance and soil-freezing.

5. Conclusions

A reanalysis data indicates that the formation mechanism of the OH clearly differs between early and late summer because it changes from an equivalent barotropic to a baroclinic structure with season. Thus, we assessed the influence of springtime snow cover on the formation of the August OH with the baroclinicity using an RCM. The model performed well in reproducing the August OH in 2008, and the results are useful for understanding the nature of the regional land-atmosphere climate system. The August OH develops with a distinct baroclinic structure due to increased surface heating via land-atmosphere coupling in eastern Siberia. The land-atmosphere coupling influences the amplification and maintenance of the baroclinic structure through surface heating. These results

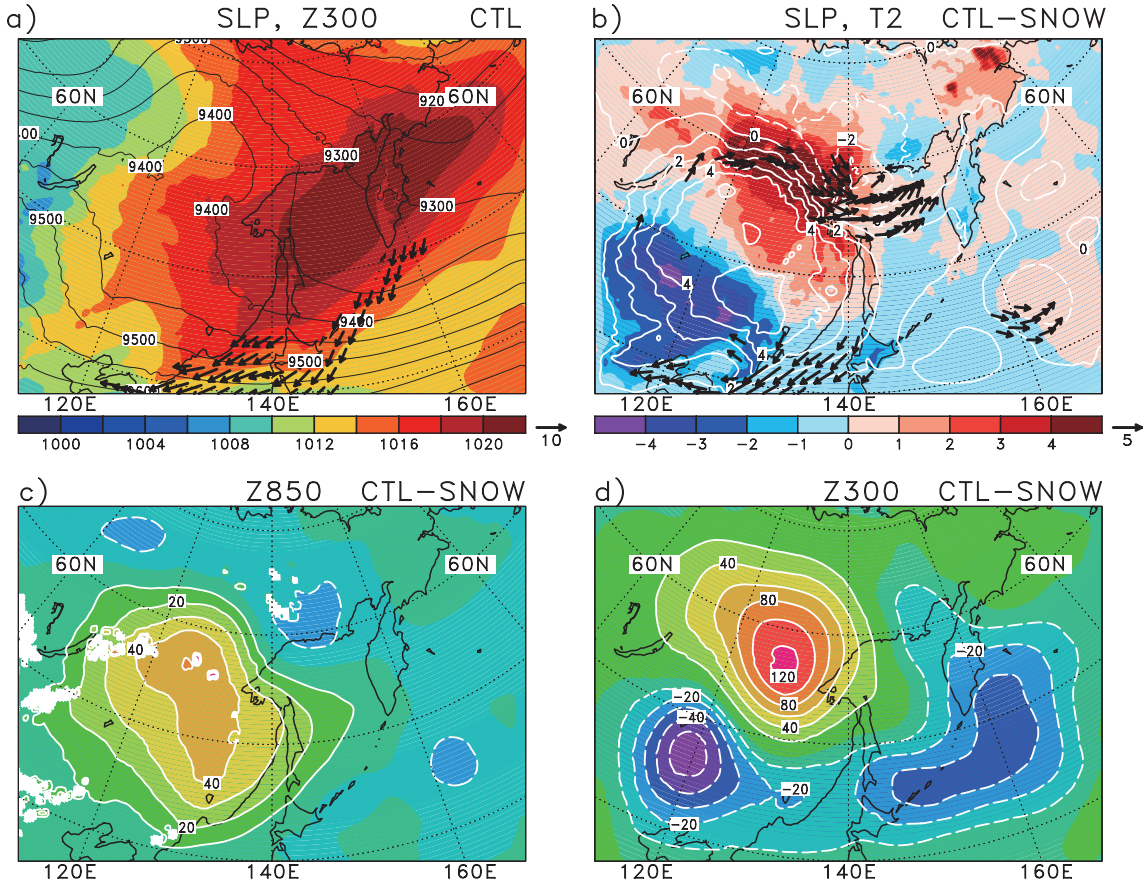

Fig. 12. As in Fig. 9, but for the period 13–27 August 2002.

suggest that the OH pressure system is not simply a regional meteorological phenomenon but a part of the land-atmosphere climate system in northern Eurasia during the warm season. We need to understand the OH as the land-atmosphere climate system without separating the atmospheric and land processes. Because soil moisture and snow cover can act as agents of climate memory at the land surface in northern Eurasia, regional land-atmosphere coupling can play a dominant role in abnormal summertime weather. However, the OH does not necessarily lead to cool summers in East Asia because tropical forcing also have influences on the variability of the OH. Further research is required to understand the OH as a climate system that involves couplings among the atmosphere, the warm land surface, and the cool ocean.

Acknowledgments

We wish to thank M. Honda for helpful support in revision. We acknowledge support from the Environment Research and Technology Development Fund (S-8-1[2]) of the Ministry of the Environment, Research Program on Climate Change Adaptation (RECCA) of the MEXT, Japan, and also the Green Network of Excellence Program (GRENE) Arctic Climate Change Research Project.

References

Arai, M., and M. Kimoto, 2005: Relationship between springtime surface temperature and early summer blocking activity over Siberia. *J. Meteor. Soc. Japan*, **83**, 261–267.

Chen, F., and J. Dudhia, 2001: Coupling an advanced land surface–hydrology model with the Penn State–NCAR MM5 modeling system. *Mon. Wea. Rev.*, **129**, 569–585.

Cohen, J., M. Barlow, P. Kushner, and K. Saito, 2007: Stratosphere-troposphere coupling and links with Eurasian land-surface variability. *J. Climate*, **20**, 5335–5343.

Delworth, T., and S. Manabe, 1989: The influence of soil

wetness on near-surface atmospheric variability. *J. Climate*, **2**, 1447–1462.

Dudhia, J., 1989: Numerical study of convection observed during the winter monsoon experiment using a mesoscale two-dimensional model. *J. Atmos. Sci.*, **46**, 3077– 3107.

Fischer, E. M., S. I. Seneviratne, P. L. Vidale, D. Lüthi, and C. Schär, 2007: Soil moisture-atmosphere interactions during the 2003 European summer heat wave. *J. Climate*, **20**, 5081–5099.

García-Herrera, R., and D. Barriopedro, 2006: Northern Hemisphere snow cover and atmospheric blocking variability. *J. Geophys. Res.*, **111**, D21104, doi:10.1029/2005JD006975.

Hong, S. Y., J. Dudhia, and S. H. Chen, 2004: A revised approach to ice microphysical processes for the bulk parameterization of clouds and precipitation. *Mon. Wea. Rev.*, **132**, 103–120.

Hong, S. Y., Y. Noh, and J. Dudhia, 2006: A new vertical diffusion package with an explicit treatment of entrainment processes. *Mon. Wea. Rev.*, **134**, 2318–2341.

Japan Meteorological Agency, 2008: Heavy rainfall in late August 2008 (in Japanese). [Available at http://www.jma.go.jp/jma/press/0809/12a/heavyrain.html.]

Kain, J. S., 2004: The Kain-Fritsch convective parameterization: An update. *J. Appl. Meteor.*, **43**, 170–181.

Kanamitsu, M., W. Ebisuzaki, J. Woollen, S.-K. Yang, J. J. Hnilo, M. Fiorino, and G. L. Potter, 2002: NCEP/DOE AMIP-II reanalysis (R-2). *Bull. Amer. Meteor. Soc.*, **83**, 1631–1643.

Matsumura, S., and K. Yamazaki, 2012: Eurasian subarctic summer climate in response to anomalous snow cover. *J. Climate*, **25**, 1305–1317.

Matsumura, S., K. Yamazaki, and T. Tokioka, 2010: Summertime land-atmosphere interactions in response to anomalous springtime snow cover in northern Eurasia. *J. Geophys. Res.*, **115**, D20107, doi:10.1029/2009JD012342.

Mlawer, E. J., S. J. Taubman, P. D. Brown, M. J. Iacono, and S. A. Clough, 1997: Radiative transfer for inhomogeneous atmospheres: RRTM, a validated correlated k model for the longwave. *J. Geophys. Res.*, **102**, 16663–16682.

Nakamura, H., and T. Fukamachi, 2004: Evolution and dynamics of summertime blocking over the Far East and the associated surface Okhotsk high. *Quart. J. Roy. Meteor. Soc.*, **130**, 1213–1233.

Ninomiya, K., and H. Mizuno, 1985a: Anomalous cold spell in summer over northeastern Japan caused by northeasterly wind from polar maritime air-mass. Part I: EOF analysis of temperature variation in relation to the largescale situation causing the cold summer. *J. Meteor. Soc. Japan*, **63**, 845–857.

Ninomiya, K., and H. Mizuno, 1985b: Anomalous cold spell in summer over northeastern Japan caused by northeasterly wind from polar maritime air-mass. Part II: Structure of the northeasterly flow from polar maritime airmass. *J. Meteor. Soc. Japan*, **63**, 858–871.

Nitta, T., 1987: Convective activities in the tropical western Pacific and their impact on the Northern Hemisphere summer circulation. *J. Meteor. Soc. Japan*, **65**, 373–390.

Numaguti, A., 1999: Origin and recycling processes of precipitating water over the Eurasian continent: Experiments using an atmospheric general circulation model. *J. Geophys. Res.*, **104**, 1957–1972.

Reynolds, R. W., N. A. Rayner, T. M. Smith, D. C. Stokes, and W. Q. Wang, 2002: An improved in situ and satellite SST analysis for climate. *J. Climate*, **15**, 1609–1625.

Sato, N., and M. Takahashi, 2007: Dynamical processes related to the appearance of the Okhotsk high during early midsummer. *J. Climate*, **20**, 4982–4994.

Skamarock, W. C., J. B. Klemp, J. Dudhia, D. M. Barker, M. G. Duda, X.-Y. Huang, Wang, and J. G. Powers, 2008: *A description of the advanced research WRF version 3*. Tech. Note NCAR/TN-475+STR, Natl. Cent. for Atmos. Res., Boulder, Colo, 113 pp.

Tachibana, Y., T. Iwamoto, M. Ogi, and Y. Watanabe, 2004: Abnormal meridional temperature gradient and its relation to the Okhotsk high. *J. Meteor. Soc. Japan*, **82**, 1399–1415.

Takata, K., and M. Kimoto, 2000: A numerical study on the impact of soil freezing on the continental-scale seasonal cycle. *J. Meteor. Soc. Japan*, **78**, 199–221.

Wakabayashi, S., and R. Kawamura, 2004: Extraction of major teleconnection patterns possibly associated with the anomalous summer climate in Japan. *J. Meteor. Soc. Japan*, **82**, 1577–1588.

Walsh, J. E., W. H. Jasperson, and B. Ross, 1985: Influence of snow cover and soil moisture on monthly air temperature. *Mon. Wea. Rev.*, **113**, 756–768.

Yabuki, H., H. Park, H. Kawamoto, R. Suzuki, V. Razuvaev, O. Bulygina, and T. Ohata, 2011: Baseline Meteorological Data in Siberia (BMDS) Version 5.0. *RIGC*. [Available at http://www.jamstec.go.jp/iorgc/cgi-bin/database/v01/browse_summary.cgi?program=hcor-&group=CDC&cat=Russia&id=BMDS_41.]

Yamada, H., 2007: Numerical simulations of the role of land surface conditions in the evolution and structure of summertime thunderstorms over a flat highland. *Mon. Wea. Rev.*, **136**, 173–188.

Yasunari, T., A. Kitoh, and T. Tokioka, 1991: Local and remote responses to excessive snow mass over Eurasia appearing in the northern spring and summer climate. *J. Meteor. Soc. Japan*, **69**, 473–487.

Yoon, J. H., and T. C. Chen, 2006: Maintenance of the boreal forest rainbelts during northern summer. *J. Climate*, **19**, 1437–1449.